

Bayesian mechanics of perceptual inference and motor control in the brain

Chang Sub Kim

Department of Physics, Chonnam National University, Gwangju 61186, Republic of Korea

E-mail: cskim@jnu.ac.kr

Abstract. The free energy principle in the neurosciences stipulates that all viable agents embody and minimize informational free energy to fit their environmental niche. We implement free energy minimization in a more physically principled manner by effectively casting it to Bayesian control dynamics. Specifically, we build a continuous-state formulation that prescribes the brain's computation for actively inferring the causes of sensory inputs, based on the principle of least action. For this, we consider that the motor signal arises from the residual errors in the cognitive expectation about the nonstationary sensory inputs at the proprioceptive level. Consequently, we derive the effective Hamilton equations that determine the optimal trajectories in the perceptual phase space, which minimize the sensory uncertainty. We also demonstrate their utility using a simple model with biological relevance to sensorimotor regulation processes such as motor reflex arcs or saccadic eye movement.

Keywords free energy principle, active inference, recognition dynamics, continuous state-space models, limit cycles

25 August 2020

1. Introduction

The free energy principle (FEP) in the field of neurosciences rationalizes that all viable organisms cognize and behave in the natural world by calling forth the probabilistic models embodied in their neural system — the brain — in a manner that ensures their adaptive fitness (Friston 2010a). The neurobiological mechanism that endows an organism’s brain — the neural observer — with this ability is theoretically framed into an inequality that weighs two information-theoretical measures, namely, the surprisal and the informational free energy (IFE) (Buckley and Kim et al. 2017). The surprisal provides a measure of the atypicality of an environmental niche, and the IFE is the upper bound of the surprisal. The inequality enables a cognitive agent to indirectly minimize the IFE as a variational objective function instead of the intractable surprisal. The minimization corresponds to inferring the external causes of afferent sensory data, encoded as a probability density at the sensory interface, e.g., sensory organs. An organism’s brain neurophysically performs the Bayesian computation of minimizing the induced IFE. This is termed as recognition dynamics (RD), which emulates — under the Laplace approximation (Buckley and Kim et al. 2017) — the predictive coding scheme of message processing or recognition (Rao and Ballard 1999).

The neurobiological mechanisms of the abductive inference of the physical brain are not yet understood; therefore, researchers mostly rely on information-theoretic concepts (Elfwing 2016; Ramstead et al. 2019; Kuzma 2019; Shimazaki 2019; Kiefer 2020, Sanders et al. 2020). The FEP facilitates dynamic causal models in the brain’s generalized-state space (Friston 2008b; Friston et al. 2010), which pose a mixed discrete-continuous Bayesian filtering (Jazwinski 1970); Balaji and Friston 2011). In the present work, we consider that the brain confronts the continuous influx of stochastic sensations and conducts the Bayesian inversion of inferring external causes in the continuous state representations. Biological phenomena are naturally continuous spatiotemporal events; accordingly, we suggest that the continuous-state approaches that are used to describe cognition and behavior are better suited than discrete-state descriptions for studying the perceptual computation in the brain. Despite its explanatory power as a unified biological principle (Friston 2013; Isomura et al. 2015; Bogacz 2017; Colombo and Wright 2018), the conventional FEP assumes several extra-theoretical facets that require evaluation. The specific issues that have drawn our attention are i) the non-Newtonian extension of dynamical states in the generalized state space and ii) the heuristic gradient-descent implementation of minimization on the instantaneous IFE landscape.

Recently, we carefully evaluated the FEP while clarifying the technical assumptions that underlie the continuous state-space formulation of the FEP Buckley and Kim et al. 2017). A full account of the discrete-state formulation, which is complementary to our formulation, can be found in (Da Costa 2020). In a subsequent study (Kim 2018), we clarified some technical facets in its conventional formalism, which necessitated a reformulation of the working hypotheses described above. In doing so, we postulated that “surprisal” plays the role of a Lagrangian in theoretical mechanics (Landau and

Lifshitz 1976; Sengupta et al. 2016), and we worked out a plausible computational implementation of the FEP by utilizing the principle of least action. Our tenet was that, although the FEP relies on the Bayesian abductive logic, it must be properly formulated and conditioned on the physical principles and laws governing the matter comprising the brain. To this end, we proposed that any process theory of the FEP ought to be based on the full implication of the inequality (Kim 2018)

$$\int dt \{-\ln p(\varphi)\} \leq \int dt \mathcal{F}[q(\vartheta), p(\varphi, \vartheta)], \quad (1)$$

where φ and ϑ collectively denote the sensory inputs and their environmental causes, respectively. The integrand on the left-hand side (LHS) of the preceding equation $-\ln p(\varphi)$ is the aforementioned *surprisal*, which measures the “self-information” contained in the sensory density $p(\varphi)$ (Cover 2006), and \mathcal{F} on the right-hand side (RHS) is the variational IFE defined as

$$\mathcal{F}[q(\vartheta), p(\varphi, \vartheta)] \equiv \int d\vartheta q(\vartheta) \ln \frac{q(\vartheta)}{p(\varphi, \vartheta)}, \quad (2)$$

which encapsulates the recognition (R-) density $q(\vartheta)$ and the generative (G-) density $p(\vartheta, \varphi)$ (see Buckley and Kim et al. 2017). While the G-density is the brain’s prior belief about the environmental dynamics and sensory generation, the R-density is the brain’s current guess of the environmental cause of the sensory perturbation. They induce variational IFE when receptors at the brain-environment interface are excited by sensory perturbations, and the induced variational IFE is encoded by the brain variables such as the action potential, synaptic plasticity, or brain waves.

According to Eq. (1), the FEP articulates that the brain minimizes the upper bound of the sensory uncertainty, which is a long-term averaged surprisal and not an instant one. We identify this bound as an informational action (IA) within the scope of the mechanical principle of least action (Landau and Lifshitz 1976). Then, by complying with the revised FEP, we derive the RD without invoking gradient-descent schemes. The RD neurophysically performs the computation for minimizing the IA when the neural observer encounters continuous streams of sensory data. The advantage of our formulation is that the brain and the environmental states are specified by using only bare continuous variables and their first-order derivatives (velocities or equivalent momenta), thereby absolving the need for the aforementioned non-Newtonian assumptions. The momentum variables represent the prediction errors, which quantify the discrepancy between an observed input and its top-down belief of a cognitive agent in the predictive coding language (Huang and Rao 2011; de Gardelle et al. 2013; Kozunov et al. 2020). In the present study, we continue our effort to make the FEP a more physically principled formalism.

The goal of this work is to extend our previous study to include the agent’s motor control, which acts on the environment to alter sensory inputs.‡ Previously, by utilizing

‡ In this work, we use the term *control*, instead of the frequently used term “action” to mean the motion of a living agent’s effectors (muscles) acting on the environment. This is done to avoid any confusion with the term *action* appearing in the nomenclature of “the principle of least action”.

the principle of least action, we focused on the formulation of perceptual dynamics for the passive inference of static sensory inputs (Kim 2018), without incorporating motor control for the active perception of nonstationary sensory streams. Here, we apply our approach to the problem of *active inference* derived from the FEP (Friston et al. 2009; Friston et al. 2010c; Friston et al. 2011a), which proposes that organisms can minimize the IFE further by altering sensory observations when the outcome of perceptual inference alone is not in accordance with an internal representation of the environment (Buckley and Kim et al. 2017). It is suggested that living systems are endowed with the ability to adjust their sensations via proprioceptive feedback, which is attributed to an inherited trait of all motile animals embodied in the reflex pathways (Tuthill and Azim 2018). In this respect, motor control is considered as an inference of the causes of motor signals that are encoded as prediction errors at proprioceptors, and motor inference is realized at the spinal level by classical reflex arcs (Friston 2011b; Adams et al. 2013). Our formulation evinces that the ensuing RD encompasses motor signals as a time-dependent source, thereby describing active inference as an extension of the optimal control theory embedding Bayesian logic (Friston 2011b; Baltieri and Buckley 2019). Another notable feature of our work is that it considers the correlation between the causal states and the sensory-data measurement, which results in significant modulation in the perceptual and motor-control outcomes.

Technically, a functional variation of the IA yields the RD that computes the Bayesian inversion, which is given as a set of coupled differential equations for the brain variables and their conjugate momenta. The brain variables are ascribed to the brain’s representation of the environmental states, and their conjugate momenta are the combined prediction errors of the sensory data and the rate of the state representations. The neural computation of active inference corresponds to integrating the RD and is subject to nonautonomous motor signals. Its solution results in optimal trajectories in the perceptual state space, which minimizes the accumulation of the IFE over continuous time, i.e., the IA. In our formulation, both descending predictions and ascending prediction errors constitute the dynamical states governed by the closed-loop RD in the functional hierarchy of the brain’s sensorimotor system. This feature is in contrast to the conventional implementation of the FEP, which considers the backward prediction — belief propagation — as neural dynamics and the forward prediction error as an instant message passing without any causal dynamics (Friston 2010a; Buckley and Kim et al. 2017).

The remainder of this paper is organized as follows. In Sect. 2, we provide a compact overview of our recent efforts in finessing the technical subtleties of the standard FEP theory. In Sect. 3, we formulate the Bayesian mechanics of the sensorimotor cycle by utilizing the principle of least action. Then, in Sect. 4, we present a parsimonious model for a concrete manifestation of our formulation. Finally, in Sect. 5, we provide the concluding remarks.

2. Outline of technical developments

Below, we recapitulate the significant developments from our continuous-state formulation, while discussing the technical features that distinguish our theory from the conventional state-space implementation of the FEP.

2.1. *Obviating the need for generalized states*

The Bayesian filtering formalism of the FEP adopts the concept of generalized motion of a physical object by defining its mechanical state beyond position and velocity (momentum). The introduction of this theoretical construct is argued to provide a more detailed specification of the dynamical states (Friston 2008a; Friston 2008b; Friston et al. 2010b). The mechanical states are generalized by recursively taking higher-order derivatives of the bare states. A point in hyperspace defined by the generalized states is interpreted as an instantaneous trajectory. This notion provides an essential theoretical basis for ensuring an equilibrium solution of the RD in the conventional formulation of the FEP (Kim 2018), and it is commonly employed by researchers (Parr and Friston 2018; Baltieri and Buckley 2019). However, the non-Newtonian construct has subtleties in assigning physical observables to higher-order motions. Standard physics does not consider jerk (third order) as a cause of the changing acceleration (second order), snap (fourth order) as a cause of the changing jerk, or the continued generalization. Instead, only the position (zeroth order) and velocity (first order) are adopted as the two required dynamical observables (Landau and Lifshitz 1976). Our formulation avoids invoking the generalized states and follows the normative rules (Kim 2018); however, it still provides a natural way to determine the equilibrium solutions for the RD. Besides, it can also handle temporal correlation, which is another justification for the conventional use of the generalized states (see Sect. 2.3).

2.2. *Replacing gradient descent implementation by the Hamiltonian mechanics*

The conventional FEP employs the gradient descent method in the optimal theory to minimize the variational IFE, i.e., the upper bound on the surprisal. To incorporate the time-varying feature of the sensory inputs, it further adopts an adroit procedure of technically distinguishing the path of a mode and the mode of a path in the generalized state space (Friston 2008b; Friston et al. 2010b). This extra-theoretical construct considers the nonequilibrium dynamics of the generalized brain states as drift-diffusion flows that locally conserve the probability density in the hyperspace of the generalized states. In the revised formulation, we replace the gradient descent scheme with the standard mechanical formulation of the least action principle (Kim 2018). The resulting novel RD entails optimal trajectories but no single fixed points in the canonical state (phase) space, which provides an estimate of the minimum sensory uncertainty, i.e., the average surprisal over a finite temporal horizon. The phase space comprises the positions (predictions) and momenta (prediction errors) of the brain's representations

of the causal environment. A recent study has indicated the necessity of exercising caution when applying gradient descent to a dynamical optimization of the objective functions in brain theory (Surace et al. 2020).

2.3. Treatment of noise correlations

The FEP requires the brain's internal model of the G-density $p(\varphi, \vartheta)$ with the likelihood $p(\varphi|\vartheta)$ and prior $p(\vartheta)$ in a top-down manner. The likelihood density is determined by the random fluctuation in the expected sensory-data generation, and the prior density is determined by that in the believed environmental dynamics. The brain encounters continuous sensory signals on a fast timescale, often shorter than the correlation time of the random processes (Friston 2008a); accordingly, in general, the noises embrace a non-Markovian stochastic process with an intrinsic temporal correlation that surmounts the ideal white-noise stochasticity. It is argued that the noises are analytic (i.e., differentiable) to allow correlation between the distinct dynamical orders of the continuous states (Friston 2008b; Friston et al. 2010b). In practice, to furnish a closed dynamics for a finite number of variables, the recursive equations of motion for the continued generalized states need to be truncated at an arbitrary order by hand. The Wiener processes with a delta-correlated (white) noise are mathematically singular; they need to be smoothed to describe fast biophysical processes. However, without resorting to the generalized states, the non-Markovian processes with colored noises can be considered within conventional stochastic theories (van Kampen:1981; Fox 1987; Risken 1989; Moon and Wettlaufer 2014). Besides, the rules of ordinary physics for a continuous motion presume the position and its first-order derivative (velocity) to be statistically uncorrelated observables at a microscopic level.

2.4. Closure of the sensorimotor loop in active inference

The conventional FEP facilitates gradient descent minimization for the mechanistic implementation of active inference, which makes the motor-control dynamics available in the brain's RD (Friston et al. 2009; Friston et al. 2010c; Friston et al. 2011a). The gradient-descent scheme is mathematically expressed as

$$\dot{a} = -\nabla_a F \rightarrow -\frac{\partial F}{\partial \varphi} \frac{d\varphi}{da}, \quad (3)$$

where a denotes an agent's motor variable, and F is the Laplace-encoded IFE by the biophysical brain variables (see Buckley and Kim et al. 2017). An agent's capability of subjecting sensory inputs to motor control is considered as a functional dependence $\varphi = \varphi(a)$ in the environmental generative processes (Friston et al. 2009). According to Eq. (3), an agent performs the minimization by effectuating the sensory data $d\varphi/da$ and obtains the best result for motor inference when $\dot{a} = 0$, where the condition $\partial F/\partial \varphi = 0$ must be met. Because $\partial F/\partial \varphi$ produces terms proportional to the sensory prediction errors, the fulfillment of motor inference is equivalent to suppressing the proprioceptive errors. Thus, the motor control tries to minimize the prediction errors,

while the prediction errors convey motor signals for the control dynamics; this forms a sensorimotor loop. Some subtle questions arise here about the dynamical status of the motor-control variable a : Equation (3) evidently handles a as a dynamical state; however, the corresponding equation of motion governing its dynamics is not given in the environmental processes. Instead, the mechanism of motor control that vicariously alters the sensory-data generation is presumed (Friston et al. 2009). In addition, motor variables are represented as the active states of the brain, e.g., motor-neuron activities in the ventral horn of the spinal cord (Friston et al. 2010c); however, they are treated differently from other hidden-state representations. Recall that the internal state representations are expressed as generalized states, whereas the active states are not.

In the following, we formulate a semi-active inference problem, which does not explicitly address motor planning in the RD but encompasses motor control as a time-dependent driving term. Our theory does not employ the theoretical construct of the generalized states and evades the gradient descent implementation of the active state dynamics. We also consider the correlation between the environmental dynamics and the generative process of sensory inputs. We regard the environmental states and the sensory variables as fluctuating, coarse-grained hydrodynamic fields, not dynamically independent microscopic states.

3. Closed-loop dynamics of perception and motion

The brain is not divided into sensory and motor systems. Instead, it is one inference machine that performs the closed-loop dynamics of perception and motor control. Here, we develop a framework of active inference within the scope of the least action principle by employing the Laplace-encoded IFE as an informational Lagrangian.

The environmental states ϑ undergo deterministic or stochastic dynamics by obeying physical laws and principles. Here, we do not explicitly consider their equations of motion because they are hidden from the brain's perspective, i.e., the brain as a neural observer does not possess direct epistemic access. Similarly, the sensory data φ are physically generated by an externally hidden process at a sensory receptor, which constitutes the brain-environment interface. However, to emphasize the effect of an agent's motor control a on sensory generation, we facilitate the generative process of sensory data, as usual, by an instantaneous mapping

$$\varphi = h(\vartheta, a) + z_{gp}, \quad (4)$$

where $h(\vartheta, a)$ is the linear or nonlinear map of the input generation, and z_{gp} is the noise involved. Note that an agent's motor-control a is explicitly included in the generative map. However, the neural observer does not know how the sensory streams are effectuated by the agent's motion in the environment (Friston et al. 2010c).

The FEP circumvents this epistemic difficulty by hypothesizing a formal homology between the external physical processes and the corresponding internal models foreseen

by the neural observer (Friston et al. 2010c). Upon receiving sensory-data influx, the brain launches the R-density $q(\vartheta)$ to infer the external causes via variational Bayes. The R-density is the probabilistic representation of the environment, whose sufficient statistics are assumed to be encoded by neurophysical brain variables, e.g., neuronal activity or synaptic efficacy. When a fixed-form Gaussian density is taken for the R-density, which is called the Laplace approximation, only the first-order sufficient statistic, i.e., the mean μ is needed to specify the IFE effectively (Buckley and Kim et al. 2017). The brain continually updates the R-density by using its internal dynamics, which is described here as a Langevin-type equation

$$\frac{d\mu}{dt} = f(\mu) + w, \quad (5)$$

where $f(\mu)$ represents the brain's belief about the external dynamics encoded by a neurophysical driving mechanism of the brain variables μ , and w is random noise. The sensory perturbations at the receptors are predicted by the neural observer via the instantaneous mapping

$$\varphi(a) = g(\mu) + z, \quad (6)$$

where the belief $g(\mu)$ is encoded by the internal variables, and z is the associated noise. Our sensory generative model provides a mechanism for sampling the sensory data φ by using the brain's active states a , which represent an external motor control embedded in Eq. (4). Note that Eq. (4) describes the environmental processes that generate sensory inputs φ , while its homolog 'Eq. (6)' prescribes the brains' prior belief about φ that can be altered by the active states a . The instantaneous state of the brain μ , which is specified by Eq. (5), picks out a particular R-density $q(\vartheta)$ when the brain seeks the true posterior (the goal of perceptual inference). The motor control fulfills the prior expectations by modifying the sensory generation via active-state effectuation at the proprioceptors.

Through Laplace approximation (Buckley and Kim et al. 2017), the G-density $p(\varphi, \vartheta)$ is encoded in the brain as $p = p(\varphi, \mu)$, where the sensory stimuli φ are predicted by the neural observer μ via Eq. (6). Here, we argue that the physical sensory-recording process is conditionally independent of the brain's internal dynamics; however, the brain states must be neurophysically involved in computing the sensory prediction. In other words, the sensory perturbation φ at the interface is a source for exciting the neuronal activity μ . This observation renders the set of Eqs. (5) and (6) to be dynamically coupled, not conditionally independent. We incorporate this conditional dependence into our formulation by introducing a correlation between the noises w and z .

For simplicity, we consider the stationary Gaussian processes for the bivariate variable Z as a column vector

$$Z \equiv \begin{pmatrix} w \\ z \end{pmatrix},$$

where $w = \dot{\mu} - f(\mu)$ and $z = \varphi - g(\mu)$, and specify the Laplace-encoded G-density $p(\varphi, \mu)$ as

$$p(\varphi, \mu) = \frac{1}{\sqrt{(2\pi)^2 |\Sigma|}} \exp\left(-\frac{1}{2} Z^T \Sigma^{-1} Z\right), \quad (7)$$

where Z^T is the transpose of Z . The covariance matrix Σ for the above is given as

$$\Sigma = \begin{pmatrix} \sigma_w & \phi(t) \\ \phi(t) & \sigma_z \end{pmatrix},$$

where the stationary variances σ_i ($i = w, z$) and the transient covariance ϕ are defined, respectively, as

$$\sigma_w(0) = \langle w^2 \rangle, \quad \sigma_z(0) = \langle z^2 \rangle, \quad \text{and} \quad \phi(t) = \langle w(0)z(t) \rangle.$$

With the prescribed internal model of the brain for the G-density, the Laplace-encoded IFE can be specified as $F(\varphi, \mu) = -\ln p(\varphi, \mu)$ (for details, see Buckley and Kim et al. 2017). Then, it follows that

$$\begin{aligned} F(\varphi, \mu; t) &= \frac{1}{2} m_w (\dot{\mu} - f(\mu))^2 + \frac{1}{2} m_z (\varphi - g(\mu))^2 \\ &\quad - \sqrt{m_w m_z} \rho (\dot{\mu} - f(\mu)) (\varphi - g(\mu)) + \frac{1}{2} \ln (2\pi(1 - \rho^2) \sigma_w \sigma_z), \end{aligned} \quad (8)$$

where ρ is the correlation function defined as a normalized covariance

$$\rho \equiv \frac{\phi}{\sqrt{\sigma_w \sigma_z}}. \quad (9)$$

We also introduce the notations m_i ($i = w, z$) as

$$m_i \equiv \frac{1}{\sigma_i(1 - \rho^2)}, \quad (10)$$

which are *precisions*, scaled by the correlation, in the conventional FEP.

Next, as we proposed in (Kim 2018), we identify F as an informational Lagrangian L in the scope of the principle of least action, and define

$$L \equiv \frac{1}{2} m_w (\dot{\mu} - f(\mu))^2 + \frac{1}{2} m_z (\varphi - g(\mu))^2 - \sqrt{m_w m_z} \rho (\dot{\mu} - f(\mu)) (\varphi - g(\mu)), \quad (11)$$

which is viewed as a function of μ and $\dot{\mu}$ for the given sensory inputs $\varphi(t)$, i.e., $L = L(\mu, \dot{\mu}; \varphi)$. Note that we dropped the last term in Eq. (8) when translating F into L because it can be expressed as a total time-derivative term that does not affect the resulting equations of motion (Landau and Lifshitz 1976). Then, the theoretical action S that effectuates the variational objective functional under the revised FEP is set up as

$$S[\mu(t)] = \int F(\mu(t), \dot{\mu}(t); \varphi) dt. \quad (12)$$

The Lagrange equation of motion, which determine the trajectory $\mu = \mu(t)$ for a given initial condition $\mu(0)$, is derived by minimizing the action $\delta S \equiv 0$.

Equivalently, the equations of motion can be considered in terms of the position μ and its conjugate momentum p , instead of the position μ and velocity $\dot{\mu}$. We have used

the terms position and velocity as a metaphor to indicate the dynamical variables μ and $\dot{\mu}$, respectively. For this, we need to convert the Lagrangian L into the Hamiltonian H by performing a Legendre transformation

$$H(\mu, p) = p\dot{\mu} - L(\mu, \dot{\mu}),$$

where p is the canonical momentum conjugate to μ , which is calculated from L as

$$p = \frac{\partial L}{\partial \dot{\mu}} = m_w(\dot{\mu} - f) - \sqrt{m_w m_z}(\varphi - g)\rho. \quad (13)$$

After some manipulation, the functional form of H can be obtained explicitly as follows

$$H(\mu, p; \varphi) = T(\mu, p; \varphi) + V(\mu; \varphi), \quad (14)$$

where we have indicated its dependence on the sensory influx φ . In addition, the terms T and V on the RHS are defined as

$$T(\mu, p; \varphi(t)) \equiv \frac{p^2}{2m_w} + \left(\rho \sqrt{\frac{m_z}{m_w}} (\varphi - g(\mu)) + f(\mu) \right) p, \quad (15)$$

$$V(\mu; \varphi(t)) \equiv \frac{1}{2} m_z (1 - \rho^2) (\varphi - g(\mu))^2. \quad (16)$$

Here, T and V represent the *kinetic and potential energies*, respectively, which define the informational Hamiltonian of the brain. Similarly, m_w and m_z represent the *neural inertial masses*, again as a metaphor. Unlike that in standard mechanics, the second term in the expression for kinetic energy is dependent on the linear momentum and position.

Next, we generate the Hamilton equations of motion, which are equivalent to the Lagrange equation, by carrying out

$$\dot{\mu} = \frac{\partial H}{\partial p} \quad \text{and} \quad \dot{p} = -\frac{\partial H}{\partial \mu}.$$

As described below, the Hamilton equations are better suited for our purposes, since they specify the RD as coupled first-order differential equations of the brain state μ and its conjugate momentum p . In contrast, the Lagrange equation is a second-order differential equation of the state variable (Landau and Lifshitz 1976). The results are as follows:

$$\dot{\mu} = \frac{1}{m_w} p + f(\mu) + \alpha \Delta_\varphi, \quad (17)$$

$$\dot{p} = -\left(\frac{\partial f}{\partial \mu} - \beta \frac{\partial g}{\partial \mu} \right) p - (1 - \gamma^2) \frac{\partial g}{\partial \mu} \Delta_\varphi, \quad (18)$$

where the parameters α , β , and γ have been respectively defined for notational convenience as

$$\alpha \equiv \rho / \sqrt{m_z m_w}, \quad \beta \equiv \rho \sqrt{m_z / m_w}, \quad \text{and} \quad \gamma \equiv \rho \sqrt{m_w / m_z}. \quad (19)$$

In Eqs. (17) and (18), we have also defined the notation Δ_φ as

$$\Delta_\varphi(\mu; t) \equiv m_z(\varphi(a) - g(\mu)). \quad (20)$$

It measures the discrepancy between the adjustable sensory input φ by an agent's motor control a and the top-down neural prediction $g(\mu)$, weighted by the neural inertial mass m_z .

Below, we appraise the Bayesian mechanics prescribed by Eqs. (17) and (18) and note some significant aspects:

- (i) The derived RD suggests that both the brain activities μ and their conjugate momenta p are dynamic variables. The instantaneous values of μ and p correspond to a point in the brain's perceptual state space, and the continuous solution over a temporal horizon forms an optimal trajectory that minimizes the theoretical action, which represents the sensory uncertainty.
- (ii) The canonical momentum p defined in Eq. (13) can be rewritten as $p = m_w(\dot{\mu} - f) - \rho\sqrt{m_w/m_z}\Delta_\varphi$. Accordingly, when the normalized correlation ρ is nonvanishing, the momentum quantifies the combined errors in predicting the changing states and the sensory stimuli. The prediction errors propagate through the brain by obeying the coupled dynamics according to Eqs. (17) and (18).
- (iii) The terms involving the time-dependent Δ_φ in Eqs. (17) and (18) are identified as the driving forces \mathcal{C}_i , $i = \mu, p$,

$$\mathcal{C}_\mu \equiv \alpha\Delta_\varphi, \quad (21)$$

$$\mathcal{C}_p \equiv -\frac{\partial V}{\partial \mu} = -(1 - \gamma^2) \frac{\partial g}{\partial \mu} \Delta_\varphi. \quad (22)$$

The sensory prediction error Δ_φ , defined in Eq. (20), quantifies the motor signals engaging with the brain's nervous control in integrating the RD.

Equations (17) and (18) are the highlights of our formulation, which prescribes the brain's Bayesian mechanics of actively inferring the external causes of sensory inputs under the revised FEP. Note that the motor variable a is not explicitly included in our derived RD; instead, it implicitly induces nonautonomous sensory inputs $\varphi(t)$ in the motor signal Δ_φ . The motor signal appears as a time-dependent driving term, which makes the RD more akin to the motor-control dynamics. The driving forces are primarily induced by the discrepancy between the sensory streams $\varphi(t)$ and those predicted by the brain. The neural observer continuously integrates the RD subject to a motor signal to perform the sensory-uncertainty minimization, thereby closing the perception and motion control within a reflex arc. When we neglect the correlation ρ between the sensory perturbation and the neuronal response to it, we can recover the RD that was reported in the previous publication (Kim 2018), which demonstrates the consistency of our formulation. The full implication of our formulation in the hierarchical brain can be straightforwardly made as done in (Kim 2018), which admits the bidirectional facet in information flow of descending predictions and ascending prediction errors (Markov and Kennedy 2013; Michalareas et al. 2016).

4. Simple Bayesian-agent model: an implicit motor control

In this section, we numerically demonstrate the utility of our formulation using an agent-based model, which is based on an early publication (Buckley and Kim et al. 2017). Unlike that in the previous study, the current model does not employ generalized states and their motions; instead, the RD is specified using only the position μ and its conjugate momentum p for a given sensory input $\varphi(t)$. The environmental objects invoking an agent's sensations can be either static or time-dependent, and in turn, the time dependence can also be either stationary (not moving on average) or nonstationary. According to the framework of active inference, the inference of static properties corresponds to passive perception without motor control a . Meanwhile, the inference of time-varying properties renders an agent's active perception of proprioceptive sensations by discharging motor signals Δ_φ via classic reflex arcs.

In the present simulation, the external hidden state ϑ is a point property, e.g., temperature or a salient visual feature, which varies with the field point x unless the environment is in global thermal equilibrium. As the simplest environmental map, we take $h(\vartheta, a) = \vartheta(x(a))$ and assume that the sensory influx at the corresponding receptor is given by

$$\varphi = \vartheta + z_{gp}, \quad (23)$$

where z_{gp} is the random fluctuation. The external property, e.g., temperature, is assumed to display a spatial profile as follows:

$$\vartheta(x) = \vartheta_0/(x^2 + 1),$$

where ϑ_0 is the value at the field origin, and the desired environmental niche is situated at $x = x_d$, where $\vartheta(x_d) = \vartheta_d$. The biological agent that senses temperature is allowed to navigate through a one-dimensional environment by exploiting the hidden property. The agent initiates its motion from $x(0)$, where the temperature does not accord with the desired value. In this case, the agent must fulfill its allostasis at the cost of biochemical energy by exploiting the environment according to

$$x(t) = x(0) + \int_0^t a(t') dt', \quad (24)$$

where $a(t)$ is a motor variable, e.g., agent's velocity. Accordingly, the nonstationary sensory data $\varphi(t)$ are afferent at the receptor with respect to the noise z_{gp} . The time dependence is caused by the agent's own motion, i.e., $\varphi(t) = \vartheta(x(a(t)))$, which is assumed to be latent to the agent's brain in the current model. With the prescribed sensorimotor control, the rate of averaged sensory data with respect to the noise is related to the control variable as follows:

$$\dot{\varphi} = \frac{\partial \varphi(x)}{\partial x} a.$$

As discussed in Sect. 3, the neural observer does not know how the sensory inputs at the proprioceptor are affected by the agent's motor reflex control. In the case of saccadic motor control (Friston et al. 2012), an agent may as well stand at a field point

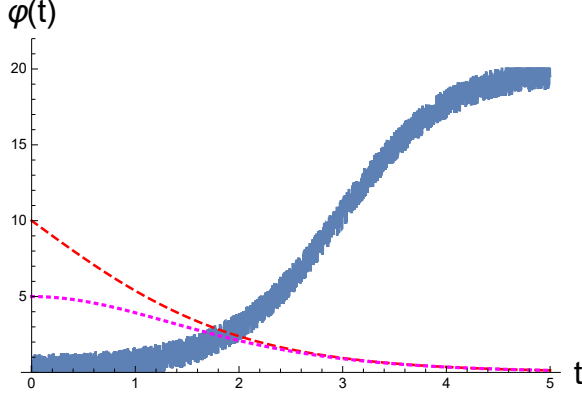


Figure 1. Influx of stochastic sensory data $\varphi(t)$ generated by the environmental process Eq. (23), where we have set $\vartheta_0 = 20$. The dashed curve represents the agent’s position $x(t)$ as a function of time, with its movement starting from $x(0) = 10$. The dotted curve represents the magnitude of the latent motor variable $a(t)$ that controls the agent’s location. [All curves are in arbitrary units.]

without changing its position but sampling the salient visual features of the environment through a fast eye movement $a(t)$, which makes the visual input nonstationary, i.e., $\varphi(t) = \vartheta(a(t))$.

In Fig. 1, we depict the streams of sensory data at the agent’s receptor as a function of time. For this simulation, the latent motor variable in Eq. (24) is taken as §

$$a(t) = a(0) \frac{e^t}{(1 + e^t)^2},$$

which renders the agent’s position in the environment as $x(t) = 2x(0)/(1 + e^t)$ with $x(0) = -2a(0)$. The figure shows that the agent, initially located at $x(0) = 10$, senses an undesirable stimulus $\vartheta(0) \doteq 0.2$; accordingly, it reacts by using motor control to find an acceptable ambient niche. After a period of $\Delta t = 5$, the agent finds itself at the origin $x = 0$, where the environmental state is marked by the value $\vartheta \doteq 20$.

Having prescribed the nonstationary sensory data, we now set up the Bayesian mechanics to be integrated by applying Eqs. (17) and (18) to the generative models below. We assume that the agent has already learned an optimal generative model; therefore, the agent retains prior expectations about the observations and dynamics. Here, for demonstrational purposes, we take the learned generative model in its simplest linear form:

$$g(\mu) = \mu, \tag{25}$$

$$f(\mu) = -(\mu - \vartheta_d). \tag{26}$$

Note that the motor control a is not included in the generative model, and the desired sensory data ϑ_d , e.g., temperature, appears as the brain’s prior belief about the hidden

§ For simplicity, we assume that this is hardwired in the agent’s reflex pathway over evolutionary and developmental time scales.

state. Accordingly, Eqs. (17) and (18) are reduced to a coupled set of differential equations for the brain variable μ and its conjugate momentum p :

$$\dot{\mu} = -(\mu - \vartheta_d) + \frac{1}{m_w} p + \alpha \Delta_\varphi, \quad (27)$$

$$\dot{p} = (1 + \beta)p - (1 - \gamma^2) \Delta_\varphi. \quad (28)$$

The parameters α , β , and γ are proportional to the correlation ρ ; see Eq. (19). Hence, they become zero when the neural response to the sensory inputs is uncorrelated with the neural dynamics, which is not the case in general. The time-dependent driving terms appearing on the RHS of both equations, namely Eqs. (27) and (28), include the sensorimotor signal $\Delta_\varphi(\mu; \varphi(t))$ given in Eq. (20). The motor variable a , which drives the nonstationary inputs $\varphi(t)$, is unknown to the neural observer in our implementation.

In the following, for a compact mathematical description, we denote the brain's perceptual state as a column vector:

$$\Psi \equiv \begin{pmatrix} \mu \\ p \end{pmatrix}.$$

The vector Ψ represents the brain's current expectation μ and the associated prediction error p with respect to the sensory causes, encoded by the neuronal activities performed when encountering a sensory influx. Therefore, in terms of the perceptual vector Ψ , Eqs. (27) and (27) are expressed as

$$\frac{d\Psi}{dt} + \mathcal{R}\Psi = \mathcal{S}, \quad (29)$$

where the relaxation matrix \mathcal{R} is defined as

$$\mathcal{R} = \begin{pmatrix} 1 + \frac{\phi}{m_w} & -\frac{1}{m_w} \\ -m_z + \frac{\phi^2}{m_w} & -(1 + \frac{\phi}{m_w}) \end{pmatrix}, \quad (30)$$

and the source vector \mathcal{S} encompassing the sensory influx $\varphi(t)$ is defined as

$$\mathcal{S} = \begin{pmatrix} \vartheta_d + \frac{\phi}{m_w} \varphi \\ -(m_z - \frac{\phi^2}{m_z}) \varphi \end{pmatrix}. \quad (31)$$

Unless it is a pathological case, the steady-state (or equilibrium) solution ψ_{eq} of Eq. (29) is uniquely obtained as

$$\Psi_{eq} = \mathcal{R}^{-1}\mathcal{S} \equiv \begin{pmatrix} \mu_{eq} \\ p_{eq} \end{pmatrix}. \quad (32)$$

We find it informative to consider the general solution $\Psi(t)$ of Eq. (29) with respect to the fixed point ψ_{eq} by setting

$$\psi(t) \equiv \Psi(t) - \Psi_{eq}.$$

To this end, we seek time-dependent solutions for the shifted measure $\psi(t)$ as follows

$$\frac{d\psi}{dt} + \mathcal{R}\psi = \delta\mathcal{S},$$

where $\delta\mathcal{S} = \mathcal{S}(t) - \mathcal{S}(\infty)$. It is straightforward to integrate the above inhomogeneous differential equation to obtain a formal solution, which is given by

$$\psi(t) = e^{-\mathcal{R}t}\psi(0) + \int_0^t dt' e^{-\mathcal{R}(t-t')}\delta\mathcal{S}(t'). \quad (33)$$

Note that $\delta\mathcal{S}$ becomes zero identically for static sensory inputs; therefore, the relaxation admits simple homogeneous dynamics. In contrast, for time-varying sensory inputs, the inhomogeneous dynamics driven by the source term is expected to be predominant. However, on time scales longer than the sensory-influx saturation time τ , it can be shown that $\delta\mathcal{S} \rightarrow 0$; for instance, $\tau \doteq 5$ in Fig. 1. Therefore, in such a time scale, the inhomogeneous contribution in the relaxation diminishes even for time-varying sensory inputs, and only the homogeneous contribution is dominant for further time-development. The ensuing homogeneous relaxation can be expressed in terms of the eigenvalues λ_l and eigenvectors $\xi^{(l)}$ of the relaxation matrix \mathcal{R} as follows:

$$\psi(t) = \sum_{l=1}^2 c_l e^{-\lambda_l t} \xi^{(l)}, \quad (34)$$

where the expansion coefficients c_l are fixed by the initial conditions $\psi(0)$. The initial conditions $\psi(0)$ represent a spontaneous or resting cognitive state. In Eq. (34), the eigenvalues and eigenvectors are determined by the secular equation

$$\mathcal{R}\xi^{(l)} = \lambda_l \xi^{(l)}. \quad (35)$$

Then, the solution for the linear RD Eq. (29) is given by

$$\Psi(t) = \Psi_{eq} + \sum_{l=1}^2 c_l e^{-\lambda_l t} \xi^{(l)}, \quad (36)$$

which is exact for perceptual inference, and legitimate for active inference on timescales $t > \tau$.

Before presenting the numerical outcome, we first inspect the nature of the fixed points by analyzing the eigenvalues of the relaxation matrix \mathcal{R} given in Eq. (30). First, it can be seen that the trace of \mathcal{R} is zero, which indicates that the two eigenvalues have opposite signs, i.e., $\lambda_1 = -\lambda_2$. Second, the determinant of \mathcal{R} can be calculated as follows

$$\text{Det}(\mathcal{R}) = -(1 + \phi/m_w) + \frac{1}{m_w} (-m_z + \phi^2/m_z).$$

Therefore, if the correlation $\phi \rightarrow 0$, it can be conjectured that both eigenvalues are real. This is because $\text{Det}(\mathcal{R}) = \lambda_1 \lambda_2 \rightarrow -1 - m_z/m_w < 0$, which gives rise to $\lambda_1^2 = \lambda_2^2 > 0$ using the first conjecture. Thus, we can conclude that the two eigenvalues are real and have opposite signs. Therefore, for $\phi = 0$, the solution will be unstable. In contrast, when the correlation is retained, $\text{Det}(\mathcal{R})$ can be positive for a suitable choice of statistical parameters, namely m_w , m_z , and ϕ . In the latter case, the condition $\lambda_1 \lambda_2 > 0$ renders $\lambda_l^2 < 0$ for both $l = 1, 2$. Accordingly, λ_1 and λ_2 that have opposite signs are purely imaginary, which makes the fixed point Ψ_{eq} a *center* (Strogatz 2015). If we define $\lambda_{1,2} \equiv \pm i\omega$, the long-time solution of RD with respect to Ψ_{eq} is expressed as

$$\psi(t) = c_1 e^{i\omega t} \xi^{(1)} + c_2 e^{-i\omega t} \xi^{(2)},$$

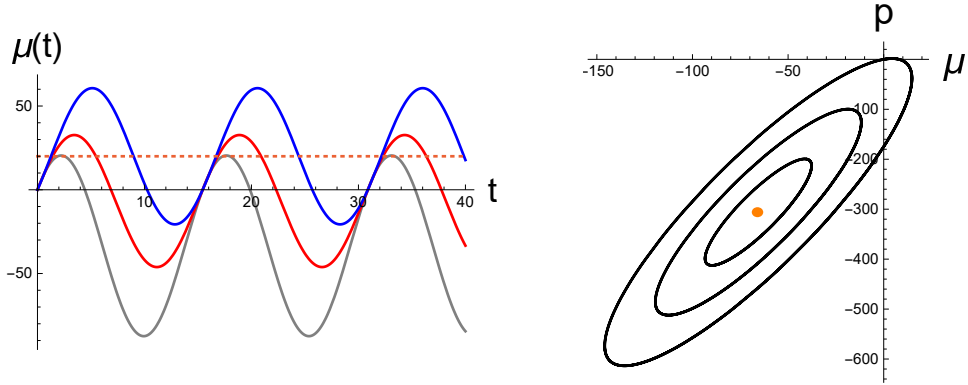


Figure 2. Perceptual inference of static sensory data: (Left) Oscillatory brain variables $\mu = \mu(t)$ developed from a common spontaneous state $(\mu(0), p(0)) = (0, 0)$ by responding to sensory inputs $\varphi = 10$ (gray), 15 (red), and 20 (blue). Horizontal dotted line indicates the agent’s prior belief about the sensory input. (Right) Limit cycles in the perceptual state space from an input $\varphi = 4.0$ for three initial conditions $(\mu(0), p(0)) = (0, 0)$, $(-20, -100)$, and $(-40, -200)$. The common fixed point is indicated by an orange bullet at the center of the orbits, which predicts the sensory cause incorrectly. [All curves are in arbitrary units.]

which specifies a limit cycle with an angular frequency ω . Thus, according to our formulation, the effect of correlation on the brain’s RD is not a subsidiary but a crucial component. Here, we consider numerical illustrations with finite correlation.

We exploited a wide range of parameters for numerically solving Eqs. (27) and (28) and found that there exists a narrow window in the statistical parameters σ_w , σ_z , and ϕ , within which a stable trajectory is allowed for a successful inference. This finding implies that the agent’s brain must learn and hardwire this narrow parameter range over evolutionary and developmental timescales; namely, the generative models are conditioned on an individual biological agent. We denote the instantaneous cognitive state as $(\mu(t), p(t))$ for notational convenience.

In Fig. 2, we present the numerical outcome from the perceptual inference of the static sensory inputs. To obtain the results, we have chosen a particular set of statistical parameters as follows:

$$\sigma_w = 1.0, \sigma_z = 10, \text{ and } \phi = -2.8,$$

which specify the neural inertial masses

$$m_w \doteq 4.6 \text{ and } m_z = 0.1 \times m_w$$

as well as the coefficients that enter the RD, namely

$$\alpha \doteq -0.60, \beta = -0.28, \text{ and } \gamma = -2.8.$$

In Fig. 2 (Left), we depict the brain variable μ as a function of time, which represents the cognitive expectation of a registered sensory input, under the generative model

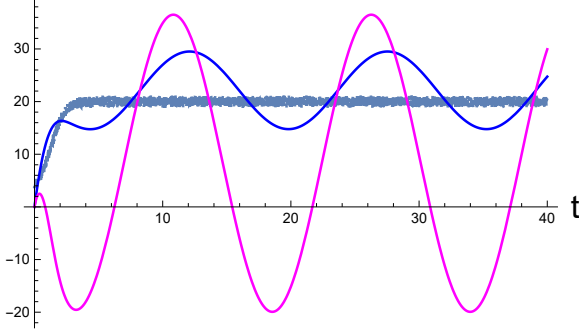


Figure 3. Active perception: Time-development of the perceptual state inferring the external causes of sensory inputs that are altered by the agent’s motor control. The blue and magenta curves depict the brain activity $\mu(t)$ and the corresponding momentum $p(t)$, respectively, and the noisy curve indicates the nonstationary sensory inputs $\varphi(t)$ at the receptor. For numerical illustration, we have used $\sigma_w = 1.0$, $\sigma_z = 10$, and $\phi = -2.8$. [All curves are in arbitrary units.]

[Eq. (25)] for three values, namely $\varphi = 10$, 15 , and 20 . For all illustrations, the agent’s prior belief with regard to the sensory input is set to be

$$\vartheta_d = 20,$$

which is indicated by the horizontal dotted line. The blue curve represents the case in which the sensory data are in line with the belief. The RD of the perceptual inference delivers an exact output $(\mu_{eq}, p_{eq}) = (20, 0)$. Note that μ_{eq} and p_{eq} are the temporal averages of $\mu(t)$ and $p(t)$, respectively, in the stationary limit. The other two inferences underscore the correct answer. Figure 2 (Right) corresponds to the case of a single sensory data $\varphi = 4.0$, which the standing agent senses at the field point $x = 2$. The ensuing trajectories from all three initial spontaneous states have their *limit cycles* in the state space defined by μ and p . We numerically determined the fixed point to be $(\mu_{eq}, p_{eq}) \doteq (-65.6, -306)$ and the two eigenvalues of the relaxation matrix \mathcal{R} to be $(\lambda_1, \lambda_2) \doteq (1.84i, -1.84i)$, which are purely imaginary and have opposite signs. Again, the perceptual outcome does not accord with the sensory input; it deviates significantly.

Next, in Fig. 3, we present the results for active inference, which were calculated using the same generative parameters used in Fig. 2. The agent is initially situated at $x(0) = 2$, where it senses the sensory influx $\vartheta(0) = 4$, which does not match the desired value $\vartheta_d = 20$. Therefore, the agent reacts to find a comfortable environmental niche matching its prior belief, which generates nonstationary sensory inputs at the receptors (see Fig. 1). It can be observed that the brain variable μ initially undergoes a transient period at $t \leq 5$. The RD commences from the resting condition $(\mu(0), p(0)) = (0, 0)$ and then develops a stationary evolution. We have also numerically confirmed that the brain’s stationary prediction μ_{eq} , which is the brain’s perceptual outcome of the sensory cause, is close to but not in line with the prior belief ϑ_d . The stationary value p_{eq} is estimated to be approximately 8.0 , which is the average of the stationary oscillation of the prediction error $p(t)$.

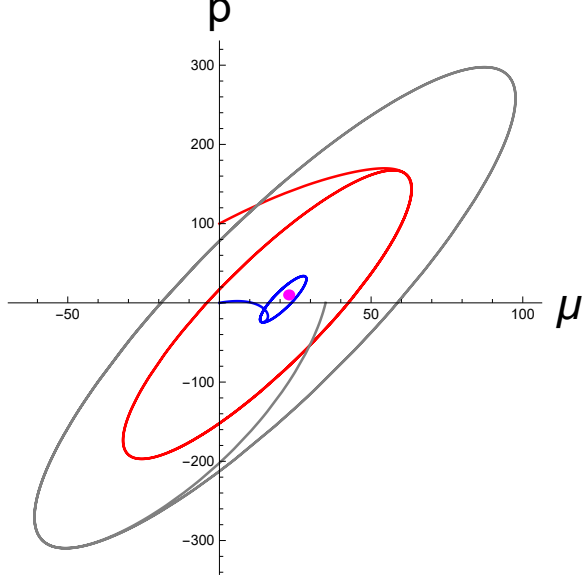


Figure 4. Active inference: Temporal development of trajectories rendering stationary limit cycles in the perceptual phase space, obtained from the same statistical parameters used in Fig. 2. The blue, red, and gray curves correspond to the three initial conditions, $(\mu(0), p(0)) = (0, 0)$, $(0, 100)$, and $(35, 0)$, respectively. The angular frequency of the limit cycles is the magnitude of the imaginary eigenvalues of the relaxation matrix \mathcal{R} given in Eq. (30). The common fixed point is indicated by a magenta bullet at the center of the orbits. [All curves are in arbitrary units.]

In Fig. 4, the trajectory corresponding to that in Fig. 3 is illustrated in blue color in the perceptual state space spanned by μ and p , including two other time developments from different choices of initial conditions. All data were calculated using the same generative parameters and sensory inputs used for Fig. 3. Regardless of the initial conditions, after each transient period, the trajectories approach stationary limit cycles about a common fixed point, as seen in the case of static sensory inputs in Fig. 2(b). The fixed point Ψ_{eq} and stationary frequency ω of the limit cycles are not affected by the initial conditions, which are solely determined by the generative parameters m_w , m_z , and ϕ and the prior belief ϑ_d for a given sensory input φ [see Eqs. (32) and (35)]. In addition, we have numerically observed that the precise location of the fixed points is stochastic, reflecting the noise from the nonstationary sensory influx φ .

In the framework of active inference, motor behavior is attributed to the inference of the causes of proprioceptive sensations (Adams et al. 2013), and in turn, the prediction errors convey the motor signals in the closed-loop dynamics of perception and motor control. In Fig. 5, we depict the sensorimotor signals $\Delta_\varphi(\mu; \varphi(t))$ that appear as time-dependent driving terms in Eqs. (27) and (28). In both figures, the agent is assumed to be initially situated in such a way as to sense the sensory data $\varphi(0) = 4$. After an initial transient period elapses, the motor signals exhibit a stationary oscillation about average zero in Fig. 5 (Left), implying the successful fulfillment of the active inference of nonstationary sensory influx matching the desired belief $\vartheta_d = 20$. The amplitude of the

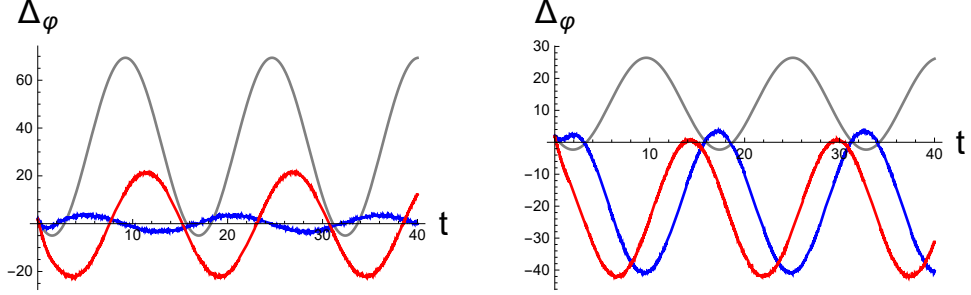


Figure 5. Motor signals $\Delta\varphi(\mu; \varphi(t))$ evoked by the discrepancy between the nonstationary sensory stream and its top-down prediction [see Eq. (20)]. Here, we set the prior belief $\vartheta_d = 20$ (Left) and $\vartheta_d = 10$ (Right). The blue and red curves represent the results from the initial condition $(\mu(0), p(0)) = (0, 0)$ and $(0, 100)$, respectively. The gray curves represent the corresponding signals from the plain perception of the static sensory input. All data were obtained by setting the statistical parameters as $\sigma_w = 1.0$, $\sigma_z = 10$, and $\phi = -2.8$. [All curves are in arbitrary units.]

motor signal shown by the blue curve is smaller than that shown by the red curve, which is also reflected in the size of the corresponding limit cycles in Fig. 4. The prediction-error signal from the plain perception also exhibits an oscillatory feature in the gray curve, which arises from the stationary time dependence of the brain variable $\mu(t)$. The amplitude shows a large variation due to the significant discrepancy between the static sensory input $\varphi = 4$ and its prior belief $\vartheta_d = 20$. In Fig. 5 (Right), for comparison, we have repeated the calculation with another value: $\vartheta_d = 10$. In this case, the prior belief ϑ_d about the sensory input does not accord with the stationary sensory streams. Therefore, the blue and red signals for active inference oscillate about the negatively shifted values from average zero. In contrast to Fig. 5 (Left), the error-signal amplitude of the static input is reduced because the difference between the sensory data and the prior belief decreases.

Next, we consider the role of correlation ϕ in the brain's RD, whose value is limited by the constraint $|\phi| \leq \sqrt{\sigma_w \sigma_z}$. To this end, we chose three values of ϕ for the fixed variances σ_w and σ_z , and integrated the RD for active inference. In Fig. 6, we present the resulting time evolution of the brain states μ for the initial condition $(\mu(0), p(0)) = (0, 0)$. In this figure, the conjugate momentum variables are not shown. The noticeable features in the results include the changes in the fixed point and the amplitude of the stationary oscillation with correlation. The average value of $\mu(t)$ in the periodic oscillation corresponds to the perceptual outcome μ_{eq} of the sensory data in the stationary limit. We remark that for all numerical data presented in this work, we have chosen only negative values for ϕ . This choice was made because our numerical inspection revealed that positive correlation does not yield stable solutions.

As the final numerical manifestation, in Fig. 7, we show the temporal buildup of the limit cycles in the perceptual phase space; however, this time, we fix σ_w while varying σ_z and ϕ . The resulting fixed points are located approximately at the center of each

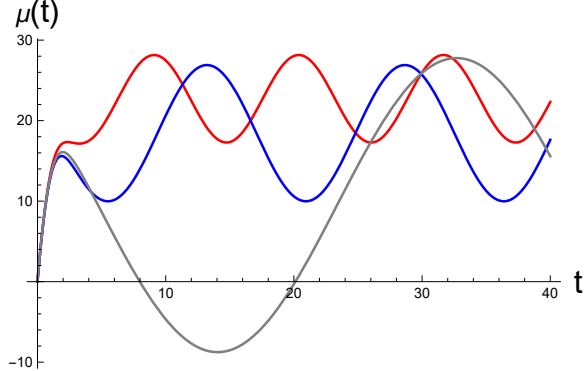


Figure 6. Time evolution of the brain variable μ . Here, we vary the correlation ϕ for fixed variances $\sigma_w = 1.0$ and $\sigma_z = 10$. The red, blue, and gray curves correspond to $\phi = -3.0$, -2.8 , and -2.6 , respectively. For all data, the agent is environmentally situated at $x = 2$, where it senses the transient sensory inputs $\varphi(t)$ induced by the motor reflexes at the proprioceptive level. The agent’s initial cognitive state is assumed to be $(\mu(0), p(0)) = (0, 0)$, and the prior belief is set as $\vartheta_d = 20$. [All curves are in arbitrary units.]

limit cycle, which are not shown. Similar to that in Fig. 6, it can be observed that the positions of the fixed point and the amplitudes of oscillation are altered by the variation in the statistical parameters. Evidently, a different set of parameters, namely σ_w , σ_z , and ϕ , which are the learning parameters encoded by the brain, result in a distinctive Bayesian mechanics of active inference.

Here, we summarize the major findings from the application of our formulation to the simple nonstationary model. The brain’s Bayesian mechanics, i.e., Eqs. (27) and (28), employ the linear generative models given in Eqs. (25) and (26).

- (i) The steady-state solutions of the RD turn out to be a center about which stationary limit cycles (periodic oscillations) are formed in the perceptual phase space, which constitute the brain’s nonequilibrium resting states.
- (ii) The nonequilibrium stationarity stems from the pair of purely imaginary eigenvalues of the relaxation matrix with opposite signs, given by Eq. (30); the magnitude specifies the angular frequency of the periodic trajectory.
- (iii) The centers are determined by the generative parameters and the prior belief for a given sensory input in the steady limit [see Eq. (32)], which represents the outcome of active inference and the entailed prediction error.
- (iv) The inclusion of noise correlation between the brain’s expectation of the external dynamics and sensory generation is consequential to ensuring a stable solution. Furthermore, based on numerical experience, a negative correlation is a prerequisite for obtaining stable solutions using the current model.

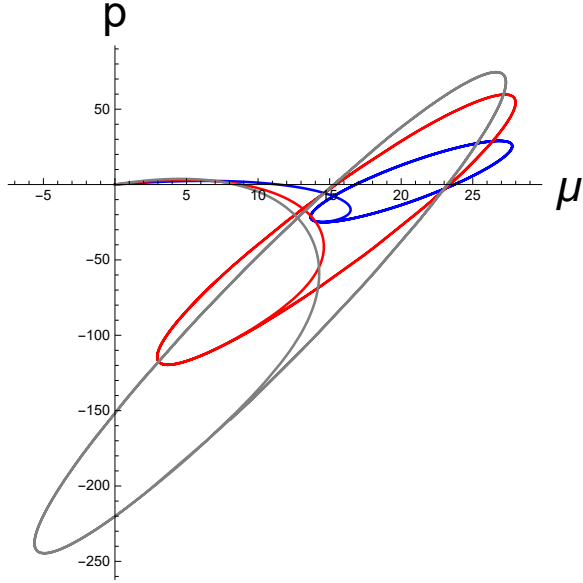


Figure 7. Limit cycles in the perceptual phase space. Here, we have considered several sets of σ_z and ϕ for a fixed $\sigma_w = 1.0$. The red, blue, and gray curves were obtained from $(\sigma_z, \phi) = (50, -6.6)$, $(10, -2.8)$, and $(100, -9.5)$, respectively. For all data, the agent's initial cognitive state is assumed to be $(\mu(0), p(0)) = (0, 0)$, and the prior belief is set as $\vartheta_d = 20$. The agent is environmentally situated at $x = 2$, where it senses the transient sensory inputs $\varphi(t)$ induced by the motor reflexes at the proprioceptive level. [All curves are in arbitrary units.]

5. Concluding remarks

We implemented the FEP with the minimization scheme derived from the principle of least action to cast the promising unified biological framework to a more physically grounded approach. It should be noted that in our theory, the continuous time-integral of the induced IFE in the brain, not an instantaneous IFE, performs as a variational objective function over a finite temporal horizon. To present the novel aspects of our formulation as well as a manifestation of its utility with a concrete model, this study focused on the perceptual inference of nonstationary sensory influx at the interface. The nonstationary sensory inputs were assumed to be unknown or contingent to the neural observer without explicitly engaging in motor-inference dynamics in the RD; in other words, the agent's sensorimotor selection was not part of our internal model. Instead, we considered that the motor signals are triggered by the discrepancies between the sensory inputs at the proprioceptive level and their top-down predictions. They appeared as nonautonomous source terms in the derived RD, thus completing the sensorimotor dynamics via reflex arcs or oculomotor dynamics of sampling visual stimuli. This closed-loop dynamics contrasts with the gradient-descent implementation, which involves the double optimization of the top-down belief propagation as well as the motor inference in the message-passing algorithms.

Using the parsimonious agent-based model, we evinced that the ensuing trajectories

and fixed points in the perceptual state space are affected by the input values of the learning parameters and the hardwired prior belief. The solutions were obtained by integrating the Bayesian equations of motion for a given default state, and they were found to be the outcome of the brain's perceptual inference of the causes of sensory stimuli. In theoretical neurosciences, it is commonly recognized that neural system dynamics implement cognitive processes that influence psychiatric states (Durstewitz et al. 2020). However, we did not attempt to explicate the effect of neural inertial masses (precisions) and correlation on the generative processes of the numerically observed limit cycles. This was because of the numerical limitation set by the presented model, which permits stable solutions in a very narrow window of statistical parameters. We hope that the key features of our manifestation will serve to motivate and guide further investigations on more realistic generative models with neurobiological implications.

Finally, we mention the recent research efforts on synthesizing perception, motor control, and decision-making within the FEP (Friston et al. 2015; Friston et al. 2017; Biel et al. 2018; Parr and Friston 2019; van de Laar and de Vries 2019; Isomura and Friston 2019; Tschantz et al. 2020; Da Costa et al. 2020). The underlying idea of these studies is rooted in machine learning, and they attempt to widen the scope of active inference by incorporating prior beliefs about behavioral policies. The new trend generalizes the instantaneous IFE F_t given in Eq. (8) to the future expected FE (EFE) in a time series and formulates the adaptive decision-making processes in action-oriented models. The EFE or generalized FE essentially appears to be a discrete sum of the informational action S in the cumulative time steps, i.e., $S \approx \sum_t F_t$ [see Eq. (12)], while encapsulating motor planning or policies as priors in the framework of Markov decision processes. The assimilation of this feature needs to be studied in depth (Millidge et al. 2020). Moreover, an inferential mechanism of motor planning for active perception can be included in the continuous-time formulation as a part of the generative models (Bogacz 2020). We are currently considering a formulation of motor planning together with the assimilation of extended IFEs in the scope of the least action principle.

References

- [1] Adams RA, Shipp S, Friston KJ (2013) Predictions not commands: active inference in the motor system. *Brain Struct Funct* 218:611–643. <https://doi.org/10.1007/s00429-012-0475-5>
- [2] Balaji B, Friston K (2011) Bayesian state estimation using generalized coordinates. *Proc. SPIE* 8050, Signal Processing, Sensor Fusion, and Target Recognition XX, 80501Y (5 May 2011); <https://doi.org/10.1117/12.883513>.
- [3] Baltieri M, Buckley CL (2019) PID control as a process of active inference with linear generative models. *Entropy* 21:257
- [4] Biehl M, Guckelsberger C, Salge C, Smith SC, Polani D (2018) Expanding the active inference landscape: More intrinsic motivations in the perception-action loop. *Front. Neurorobot* 12:45. doi: 10.3389/fnbot.2018.00045
- [5] Bogacz R (2017) A tutorial on the free-energy framework for modelling perception and learning. *Journal of Mathematical Psychology* 76(B):198–211. <https://doi.org/10.1016/j.jmp.2015.11.003>
- [6] Bogacz R (2020) Dopamine role in learning and action inference. *eLife* 9:e53262. DOI: <https://doi.org/10.7554/eLife.53262>

- [7] Buckley CL, Kim CS, McGregor S, Seth AK (2017) The free energy principle for action and perception: A mathematical review. *Journal of Mathematical Psychology* 81:55–79. <https://doi.org/10.1016/j.jmp.2017.09.004>
- [8] Colombo M, Wright C (2018) First principles in the life sciences: The free-energy principle, organicism, and mechanism. *Synthese*. <https://doi.org/10.1007/s11229-018-01932-w>
- [9] Cover T, Thomas JA (2006) Elements of Information Theory 2nd ed. Wiley-Interscience, Hoboken
- [10] Da Costa L, Parr T, Sajid N, Veselic S, Neacsu V, Friston K (2020) Active inference on discrete state-spaces: a synthesis. *arXiv:2001.07203 [q-bio.NC]*
- [11] de Gardelle V, Waszczuk M, Egner T, Summerfield C (2013) Concurrent repetition enhancement and suppression responses in extrastriate visual cortex. *Cerebral Cortex* 23(9):2235–2244. <https://doi.org/10.1093/cercor/bhs211>
- [12] Durstewitz D, Huys Q, Koppe G (2020) Psychiatric illnesses as disorders of network dynamics. *Biological Psychiatry: Cognitive Neuroscience and Neuroimaging*. <https://doi.org/10.1016/j.bpsc.2020.01.001>
- [13] Elfwing S, Uchibe E, Doya K (2016) From free energy to expected energy: Improving energy-based value function approximation in reinforcement learning. *Neural Networks* 84:17–27. <http://dx.doi.org/10.1016/j.neunet.2016.07.013>
- [14] Fox RF (1987) Stochastic calculus in physics. *J Stat Phys* 46:11451157. <https://doi.org/10.1007/BF01011160>
- [15] Friston K (2008a) Hierarchical models in the brain. *PLoS Comput Biol* 4(11): e1000211. doi:10.1371/journal.pcbi.1000211
- [16] Friston KJ (2008b) Variational filtering. *NeuroImage* 41:747–766
- [17] Friston KJ, Daunizeau J, Kiebel SJ (2009) Reinforcement learning or active inference?. *PLoS ONE* 4(7):e6421. doi:10.1371/journal.pone.0006421
- [18] Friston K (2010a) The free-energy principle: a unified brain theory?. *Nature Reviews Neuroscience* 11:127–138
- [19] Friston K, Stephan K, Li B, Daunizeau J (2010b) Generalized filtering. *Mathematical Problems in Engineering* 2010:261670.
- [20] Friston KJ, Daunizeau J, Kilner J, Kiebel SJ (2010c) Action and behavior: a free-energy formulation. *Biol Cybern* 102(3):227260
- [21] Friston K, Mattout J, Kilner J (2011a) Action understanding and active inference. *Biol Cybern* 104:137–160.
- [22] Friston K (2011b) What is optimal about motor control?. *Neuron* 72(3):488–498. DOI 10.1016/j.neuron.2011.10.018
- [23] Friston K, Adams R, Perrinet L, Breakspear M (2012) Perceptions as hypotheses: saccades as experiments. *Frontiers in Psychology* 3:151. <https://doi.org/10.3389/fpsyg.2012.00151>
- [24] Friston K (2013) Life as we know it. *J R Soc Interface* 10:1020130475. <http://doi.org/10.1098/rsif.2013.0475>
- [25] Friston K, Rigoli F, Ognibene D, Mathys C, Fitzgerald T, Pezzulo G (2015) Active inference and epistemic value. *Cogn Neurosci* 6:187–214. doi: 10.1080/17588928.2015.1020053
- [26] Friston KJ, Parr T, de Vries B (2017) The graphical brain: Belief propagation and active inference. *Network Neuroscience* 1(4):381414.
- [27] Huang Y, Rao RPN (2011) Predictive coding. *WIREs Cogn Sci* 2:580–593. DOI: 10.1002/wcs.142
- [28] Isomura T, Kotani K, Jimbo Y (2015) Cultured cortical neurons can perform blind source separation according to the free-energy principle. *PLoS Comput Biol* 11(12):e1004643. doi:10.1371/journal.pcbi.1004643
- [29] Isomura T, Friston K (2020) Reverse engineering neural networks to characterise their cost functions. *bioRxiv* 654467. doi: <https://doi.org/10.1101/654467>
- [30] Jazwinski AH (1970) Stochastic process and filtering theory. Academic Press, New York
- [31] Kiefer AB (2020) Psychophysical identity and free energy. *J. R. Soc. Interface* 17: 20200370. <http://dx.doi.org/10.1098/rsif.2020.0370>

- [32] Kim CS (2018) Recognition dynamics in the brain under the free energy principle. *Neural Computation* 30:2616–2659. https://doi.org/10.1162/neco_a_01115
- [33] Kozunov VV, West TO, Nikolaeva AY, Stroganova TA, Friston KJ (2020) Object recognition is enabled by an experience-dependent appraisal of visual features in the brains value system. *NeuroImage* 221:117143. <https://doi.org/10.1016/j.neuroimage.2020.117143>
- [34] Kuzma S (2019) Energy-information coupling during integrative cognitive processes. *Journal of Theoretical Biology* 469:180–186. <https://doi.org/10.1016/j.jtbi.2019.03.005>
- [35] Landau LD, Lifshitz EM (1976) Mechanics: Volume 1 (Course of Theoretical Physics S) 3rd Edition. Elsevier Ltd, Amsterdam
- [36] Markov NT, Kennedy H (2013) The importance of being hierarchical. *Curr Opin Neurobiol* 23(2):187–194. doi:10.1016/j.conb.2012.12.008
- [37] Michalareas G, Vezoli J, van Pelt S, Schoffelen JM, Kennedy H, Fries P (2016) Alpha-beta and gamma rhythms subserve feedback and feedforward influences among human visual cortical areas. *Neuron* 89(2):384–397. doi:10.1016/j.neuron.2015.12.018
- [38] Millidge B, Tschantz A, Buckley CL (2020) Whence the expected free energy?. arXiv:2004.08128 [cs.AI]
- [39] Moon W, Wettlaufer J (2014) On the interpretation of Stratonovich calculus. *New J Phys* 16:055017. <http://dx.doi.org/10.1088/1367-2630/16/5/055017>
- [40] Parr T, Friston KJ (2018) Active inference and the anatomy of oculomotion. *Neuropsychologia* 111:334–343. <https://doi.org/10.1016/j.neuropsychologia.2018.01.041>
- [41] Parr T, Friston KJ (2019) Generalised free energy and active inference. *Biol Cybern* 113:495–513. <https://doi.org/10.1007/s00422-019-00805-w>
- [42] Ramstead MJD, Constant A, Badcock PB, Friston KJ (2019) Variational ecology and the physics of sentient systems. *Physics of Life Reviews* 31:188–205. <https://doi.org/10.1016/j.plrev.2018.12.002>
- [43] Rao RPN, Ballard DH (1999) Predictive coding in the visual cortex: a functional interpretation of some extra-classical receptive-field effects. *Nature Neuroscience* 2(1):79–87. <https://doi.org/10.1038/4580>
- [44] Risken H (1989) The Fokker-Planck Equation 2nd edition. Springer-Verlag, Berlin
- [45] Sanders H, Wilson MA, Gershman SJ (2020) Hippocampal remapping as hidden state inference. *eLife* 9:e51140. <https://doi.org/10.7554/eLife.51140>
- [46] Sengupta B, Tozzi A, Cooray GK, Douglas PK, Friston KJ (2016) Towards a neuronal gauge theory. *PLoS Biol* 14(3): e1002400. <https://doi.org/10.1371/journal.pbio.1002400>
- [47] Shimazaki H (2019) The principles of adaptation in organisms and machines I: machine learning, information theory, and thermodynamics. arXiv:1902.11233
- [48] Strogatz SH (2015) Nonlinear dynamics and chaos: with applications to physics, biology, chemistry, and engineering (Studies in Nonlinearity) 2nd Edition. Westview Press, Cambridge
- [49] Surace SC, Pfister JP, Gerstner W, Brea J (2020) On the choice of metric in gradient-based theories of brain function. *PLoS Comput Biol* 16(4):e1007640. <https://doi.org/10.1371/journal.pcbi.1007640>
- [50] Tschantz A, Seth AK, Buckley CL (2020) Learning action-oriented models through active inference. *PLOS Computational Biology* 16(4):E1007805. <https://doi.org/10.1371/journal.pcbi.1007805>
- [51] Tuthill JC, Azim E (2018) Proprioception. *Current Biology* 28(5):R194–R203 doi:10.1016/j.cub.2018.01.064
- [52] van Kampen NG (1981) It versus Stratonovich. *J Stat Phys* 24:175–187. <https://doi.org/10.1007/BF01007642>
- [53] van de Laar TW, de Vries B (2019) Simulating active inference processes by message passing. *Frontiers in Robotics and AI* 6:20. <https://doi.org/10.3389/frobt.2019.00020>